



LAWRENCE
LIVERMORE
NATIONAL
LABORATORY

A Water-based Neutron Detector as a Well Multiplicity Counter

S. Dazeley, A. Asghari, A. Bernstein, N. Bowden,
V. Mozin

May 9, 2014

Nuclear Instruments and Methods in Physics Research
Section A: Accelerators, Spectrometers, Detectors and
Associated Equipment

Disclaimer

This document was prepared as an account of work sponsored by an agency of the United States government. Neither the United States government nor Lawrence Livermore National Security, LLC, nor any of their employees makes any warranty, expressed or implied, or assumes any legal liability or responsibility for the accuracy, completeness, or usefulness of any information, apparatus, product, or process disclosed, or represents that its use would not infringe privately owned rights. Reference herein to any specific commercial product, process, or service by trade name, trademark, manufacturer, or otherwise does not necessarily constitute or imply its endorsement, recommendation, or favoring by the United States government or Lawrence Livermore National Security, LLC. The views and opinions of authors expressed herein do not necessarily state or reflect those of the United States government or Lawrence Livermore National Security, LLC, and shall not be used for advertising or product endorsement purposes.

1 A Water-based Neutron Detector as a Well Multiplicity Counter

2

3 S. Dazeley^{a*}, A. Asghari^b, A. Bernstein^a, N. S. Bowden^a, V. Mozin^a

4 ^a Lawrence Livermore National Laboratory, Livermore, CA 94550, USA

5 ^b Department of Nuclear Engineering, University of California, Berkeley, CA 94720, USA

6

7 Abstract

8 We report the performance characteristics of a water-based neutron detecting multiplicity counter for the
9 non-destructive assay of fissile sources. This technique could replace or supplement existing ³He-based
10 multiplicity counters. The counter is a 1.02 m³ tank containing pure deionized water doped with 0.5%
11 GdCl₃. It has highly reflective walls and eight 10-inch PMTs mounted at the top. An unshielded source
12 well of 19 cm diameter, mounted at the top and center, extends 73 cm down into the detector. The counter
13 was evaluated using low intensity ²⁵²Cf and ⁶⁰Co sources, and a fast pulsing LED to simulate higher
14 intensity backgrounds. At low gamma ray intensities (~200 kBq or less) we report an absolute neutron
15 detection efficiency of 28% and a ⁶⁰Co rejection/suppression factor of ~10⁸ to 1. For sources with high
16 gamma ray intensities, the neutron efficiency was 22% ± 1% up to a ⁶⁰Co equivalent activity of 4 MBq.
17 The detector background event rate, primarily due to muons and other cosmogenic particles, was found to
18 be stable over a period of almost three months. The minimum detectable neutron source intensity above
19 background was 3.1 neutrons/second, assuming a one-hour data acquisition.

20

21 **Keywords:** Water Cherenkov, neutron detector, multiplicity well counter, fission, spent fuel

22

23 1. Introduction

24 In recent years the severe shortage of ³He has been a great concern for organizations involved in nuclear
25 security ([1],[2],[3]). ³He-based ionization tubes are uniquely suited for neutron detection: they are safe and
26 non-cryogenic, exploit the high neutron capture cross section of ³He, and have excellent gamma ray
27 rejection. Detector configurations comprising tightly packed arrays of ³He tubes within a moderating

* Corresponding author: Lawrence Livermore National Laboratory, 7000 East Ave, L-211, Livermore, CA, 94550. Ph: 925 423 4792, Email address: dazeley2@llnl.gov

1 material such as polyethylene are highly efficient and can be used to detect multiple neutrons arising from
2 single fissions, and hence measure the fissile content of samples of special nuclear material (e.g. [4],[5])
3 ³He-based well counting systems range in efficiency from 10% to 50%, depending on how tightly tubes are
4 packed and the ³He gas density. Highly efficient and large systems, however, require the use of a large
5 fraction of the yearly supply of ³He and are prohibitively expensive. In recent years the number of
6 competing neutron detection techniques has proliferated in response to the ³He shortage, but many are not
7 yet ready for widespread use. Boron-based systems such as BF₃ and ¹⁰B tubes/planes present toxicity
8 concerns and/or are relatively inefficient. Scintillator-based solutions often rely on differences in signal
9 pulse shape to discriminate against gamma rays, placing severe limits on the event rate that can be tolerated
10 before pileup issues dominate. Germanium or silicon-based detectors are small, reducing their overall
11 efficiency. Due to deployment of large-volume neutron detectors at US borders and increased demand for
12 medical imaging, US federal ³He reserves have decreased from 220,000 liters in 2001 to 50,000 liters in
13 2010 [2]. The cost of ³He has increased from \$45-\$85 per liter prior to the shortage to \$600-\$1000 per liter
14 in 2011. Since the ³He shortage is projected to continue for the foreseeable future, alternative techniques
15 are needed.

16

17 Coincidence counting of neutrons is an effective way to non-destructively determine the amount of fissile
18 material within a sample of special nuclear material (SNM) [6]. The technique is to measure pairs of
19 neutrons correlated in time from single fission events. For many fissile source configurations, multiplicity
20 counting is a more powerful and general technique. However, it requires detection of three or more
21 neutrons from a single fission event. Since the efficiency for detection of n coincident neutrons scales as
22 the nth power of the efficiency for one neutron, the single neutron detection efficiency quickly becomes the
23 most important criterion for evaluation of new technologies. Of the options available, despite their toxicity,
24 BF₃ gas detectors have been considered the most viable alternative to ³He for safeguards applications,
25 because of the stringent efficiency requirements [7].

26

27 In evaluating the efficacy of a neutron coincidence counting technique, the safeguards figure-of-merit

28 | (FOM) is a standard metric ([7],[8]):

1

2 $FOM = \frac{\epsilon}{\sqrt{\tau}}$.

3

4 ϵ is the single neutron detection efficiency and τ the mean thermal neutron capture time (often referred to as
5 the die-away time). A second important performance criterion is the ability of the detector to maintain high
6 neutron detection efficiency and low dead time in the presence of a high gamma ray dose rate. Dose rates
7 at the detector face may be as high as 500 mR/h for spent nuclear fuel sources [9]. High gamma ray dose
8 rates, however, are only significant in the context of a water Cherenkov detector if the gamma rays are of
9 sufficiently high energy. Extreme levels of gamma ray emission from ^{137}Cs or ^{241}Am are likely to produce
10 almost no water Cherenkov response whatsoever, as we demonstrate below.

11

12 In recent years we have studied a number of water-based detectors for the purpose of detecting neutrons
13 ([10],[11],[12]), achieving neutron efficiencies in the 20% to 30% range depending on the materials used
14 and the application. We present here an investigation into the utility of using a water-based neutron
15 detector for the purpose of non-destructive assay (NDA) of special nuclear material.

16

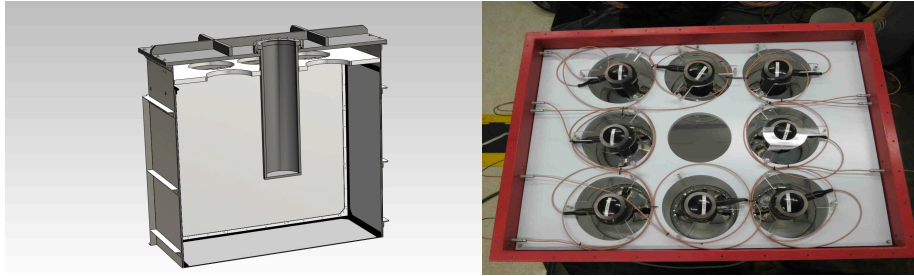
17 **2. The Water-Based Well Counter**

18

19 The active volume of the Water-Based Well Counter (WBWC) comprises 1.02 m³ of pure 18 MOhm
20 deionized water doped with 0.5% gadolinium-chloride (GdCl₃), contained within a stainless steel tank
21 (121.9 cm x 91.4 cm x 119.4 cm). To protect the doped water from the corrosive effects of chlorine on
22 stainless steel [13], the inside of the tank was coated with a baked on layer of Teflon. **Figure 1**, shows a
23 schematic and picture of the detector. There are eight waterproof Hamamatsu R7081 10-inch PMTs
24 mounted at the top of the detector looking down into the water volume. The water level is filled to half
25 way up the PMT bulbs so that they are approximately neutrally buoyant. All of the PMT supports were
26 constructed from clear acrylic or reflective white polypropylene, relatively inert polymers that do not react
27 with deionized water, to maximize the transmission and/or reflection of photons in the detector. Also
28 mounted from the top in the center is a 19 cm diameter well, or source cavity, that extends 73 cm down into

1 the tank (approximately 45 cm into the water). The well accommodates square samples as large as 15x15
2 cm². In order to efficiently transport Cherenkov photons to the PMTs the walls of the tank were also
3 coated with a 1.0 mm reflective layer of GORE® DRP®, - a Teflon-based highly reflective material (> 99%
4 in the blue and near UV).

5



6
7 Figure 1: A Schematic (left) of the detector showing a cut away of the 73 cm deep source deployment well/cavity and
8 PMT placement (PMTs not shown). To the right is the finished detector immediately after PMT placement inside and
9 prior to the installation of the lid and well.

10

11 Signals from each of the eight PMTs were sent into a CAEN V975 fast amplifier where they were
12 amplified and split, with one signal sent to a CAEN V814 discriminator and the other to a Struck SIS3320
13 waveform digitizer (WFD). The trigger was generated by a CAEN V1495 FPGA from the simultaneous
14 arrival of any three discriminator signals. Once a trigger is issued, the WFD can either record full
15 microsecond (μ s) long waveforms with a 5 nanosecond (ns) sampling interval, or digitize a set of
16 independently integrated waveform sections for each PMT.

17

18 The PMT gains were set relatively high ($\sim 10^7$) to resolve single photoelectron peaks, enabling easy gain
19 calibration via a green LED permanently mounted inside the detector.

20

21

22 3. Characteristic Response to Neutrons and Gamma Rays

23

24 Spontaneous fission sources, such as ²⁵²Cf, emit coincident gamma rays and neutrons with every fission,
25 which can result in a set of correlated events in the detector. If the fission gamma rays are of sufficient
26 energy (~ 1 MeV) and multiplicity, they may produce an instantaneous response in the WBWC. Neutrons
27 are efficiently moderated in the active water volume and preferentially capture on gadolinium. The large

1 gadolinium capture cross section results in a short mean capture time of 16 μs . When multiple gamma rays
2 and neutrons are produced simultaneously, the result is a sequence of correlated events, beginning with
3 either Cherenkov light from above-threshold gamma ray(s), or with a neutron capture (if the prompt
4 gamma rays failed to trigger the detector), and followed by delayed neutron captures. In any given
5 correlated sequence, events occurring after the first event are more likely to be neutron captures.
6 Uncorrelated event sequences may also arise, from the random arrivals of background gamma rays, or from
7 two or more different source fissions.

8

9 **Figure 2**, shows the distribution of time intervals between successive events from a one-hour calibration run
10 with a 1.0 μCi ^{252}Cf fission source placed at the base of the source cavity. The inter-event time distribution
11 has two exponential components – a fast decaying correlated component with mean inter-event time 12.3
12 μs , and an uncorrelated component with mean inter-event time of 395 μs . The short time constant

13 exponential is associated with the correlated neutron bursts of interest. This is shown in **Figure 3**, where
14 events with small inter-event times have a spectral shape enhanced at higher energies by the excess of
15 neutron captures. The underlying uncorrelated component, however, has the same spectral shape as events
16 with long inter-event times. We subtract this component using the normalization provided by the

17 exponential fit of the uncorrelated inter-event time distribution. **Figure 3**, illustrates this statistical
18 subtraction, which results in a spectrum that corresponds to the WBWC response to neutron captures on
19 gadolinium and hydrogen.

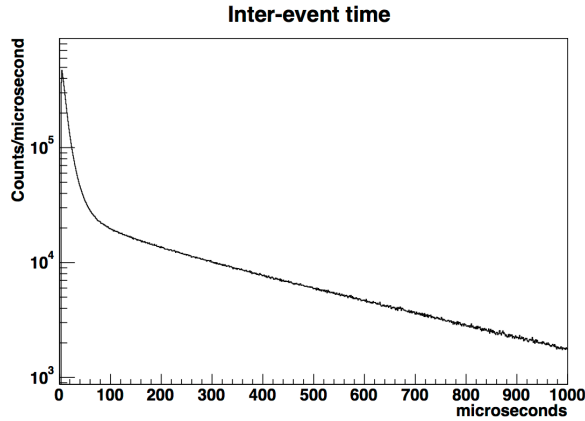
20

21

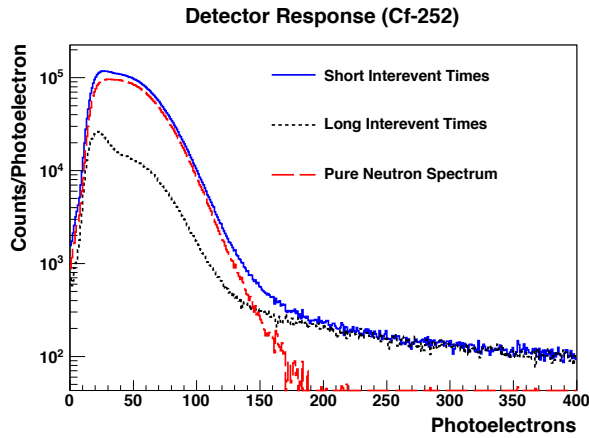
Dazeley, S
Deleted: 1

Dazeley, S
Deleted: 1

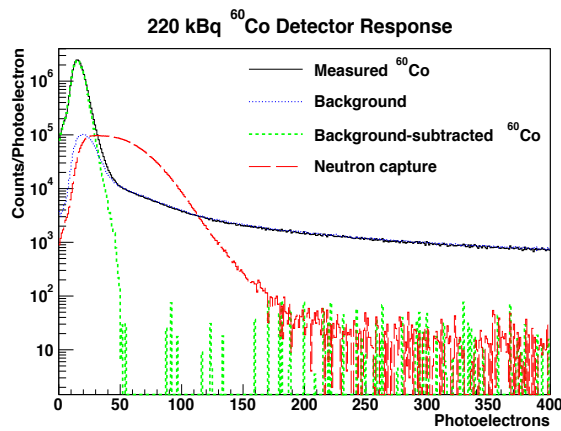
Dazeley, S
Deleted: 1



1
2
3
4
5
6
Figure 2: A plot of the inter-event time distribution for a one-hour measurement of a ^{252}Cf source in the source well/cavity. The distribution is well fit by a double exponential function – indicating a correlated and non-correlated component. The correlated component, at small inter-event times, is due to the thermalization and capture of multiple simultaneously emitted neutrons in the detector. Its exponential has a time constant consistent with a mean inter-event time of 12.3 μs .



7
8
9
10
11
Figure 3: A comparison of the charge spectrum for event pairs with short inter-event times and long inter-event times. In both datasets the number of uncorrelated events is the same. The statistical subtraction of the two, which gives the background free spectrum of neutron capture events, is also shown.



12
13
14
Figure 4: The detector spectral response of a 220 kBq ^{60}Co source for a one-hour data acquisition. Also shown is a one-hour background run, and the background subtracted ^{60}Co response. Shown for comparison is the “pure” neutron capture spectral response that was generated in Figure 3.

1
2
3
4
5
6
7
8
9
10
11
12
13

Figure 4 shows the spectral response of the detector to a 220 kBq (5.9 μ Ci) ^{60}Co source positioned inside the well for a one hour data acquisition (red), compared to a one-hour background run (black, no source). The blue curve shows the background subtracted “pure” ^{60}Co spectral response. The ^{60}Co source was used as a proxy for any kind of source that emits a low intensity gamma ray background at an energy of approximately 1 to 2 MeV. Also shown for comparison is the “pure” neutron capture spectrum generated in **Figure 3**. By requiring a selection criterion of at least 50 photoelectrons it is possible to remove all evidence of the ^{60}Co background while maintaining high neutron detection efficiency.

Dazeley, S
Deleted: 1

Dazeley, S
Deleted: 1

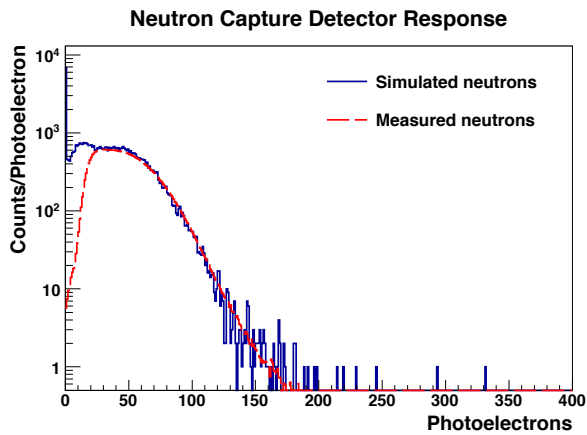


Figure 5: A comparison of the simulated and real data neutron capture spectrum after tuning.

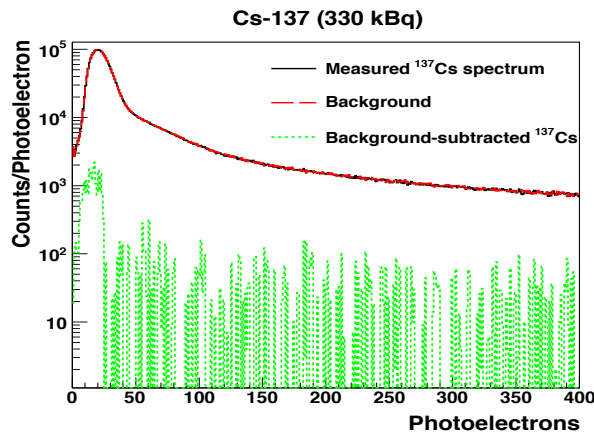
14
15
16
17
18
19
20
21
22
23
24
25

To obtain the neutron detection efficiency we constructed a GEANT4 [14],[15],[16] model of our detector, tuned to reproduce the background free neutron capture spectral response. **Figure 5** shows a comparison of the simulated and measured neutron spectra. The two distributions agree very well above about 25 photoelectrons. Below 25 photoelectrons they diverge due to detector threshold effects which are not modeled in the simulation. The only parameters tuned were water attenuation length, wall reflectivity and average PMT quantum efficiency. In our model, the average wall reflectivity was set to 93% - this was a simplification of the real detector, which comprised side and base walls, covered in GORE DRP (99%), and polypropylene between the PMTs at the top and around the edges of the detector, assumed to be approximately 80% reflective. The water attenuation length was modeled by a function that reaches a

Dazeley, S
Deleted: 1

1 maximum of about 35 meters. The functional shape was taken from a measurement at Super-Kamiokande
2 [17]. The PMT quantum efficiency (QE) was modeled using data supplied by the manufacturer. To
3 account for the fact that the PMTs were not magnetically shielded the QE was multiplied by a factor of
4 0.85.

5
6



7
8 Figure 6: A one-hour ^{137}Cs data acquisition compared to a one-hour no-source background run. Note they are almost
9 identical. The statistical subtraction represents the background subtracted ^{137}Cs detector response.

10 The simulated neutron source, like the real one, was located at the base of the source well. For simplicity
11 the neutron energy was a constant 1 MeV, since the input neutron energies have little impact on the
12 resulting neutron capture spectrum. Including all of the neutrons emitted from the source, and selecting
13 only events between 50 and 200 photoelectrons, we obtain an absolute neutron detection efficiency of 28%.
14 This efficiency represents the fraction of simulated neutrons that produce a response in the detector
15 between 50 and 200 photoelectrons. The efficiency was also calculated simply from the nominal ^{252}Cf
16 source activity, last measured in October 2007 at 185 kBq. The uncertainty associated with this activity is
17 unknown, but typically manufacturers quote approximately 10% uncertainty for check sources of this type.
18 Our measurements were made approximately 6 years (2.26 half lives) later, implying source intensity of 38
19 ± 4 kBq (1.0 μCi). The WBWC detected 1230 neutrons out of a possible 4400 per second, at an efficiency
20 of $28 \pm 3\%$, in excellent agreement with the predicted value from simulation.

21

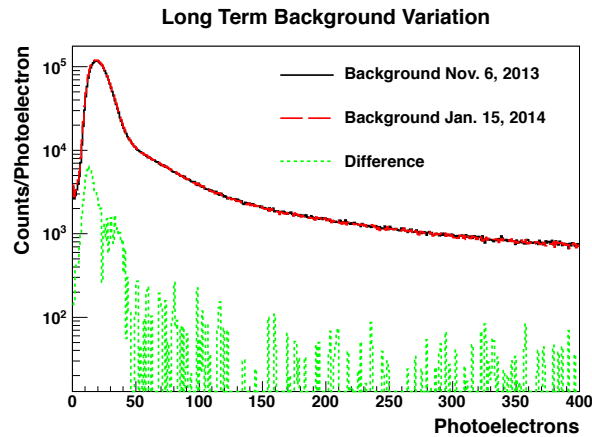
22 | **Figure 6**, shows the detector response spectrum from a one hour run using a 338 kBq (9.2 μCi) ^{137}Cs source,
23 compared with a no source run of the same duration. It shows an attractive feature of Cherenkov detectors,
24 namely the inherent insensitivity to low energy (662 keV) gamma rays from ^{137}Cs , a major isotope present

1 in spent nuclear fuel, since Compton scattering results in few electrons above the Cherenkov threshold (260
2 keV). Note that the only significant response from the detector is below 25 photoelectrons, and even then
3 the trigger rate as a result of the 338 kBq ^{137}Cs source was less than 10 Hz.

4

5 In [Figure 4](#) and [Figure 6](#), the background spectra were obtained with no radioactive sources present. Over
6 the energy range we use to select neutron capture events (50 to 200 photoelectrons), the background event
7 rate was approximately 155 Hz. Both the background rate and the spectral response of the detector have
8 remained remarkably constant over the full period of data taking. **Figure 7** illustrates this point, with one-
9 hour background runs taken on November 6 2013 and January 15 2014. The difference between them is
10 also shown. Over that time period the neutron background event rate dropped only slightly, from 155
11 (± 0.2) to 154.8 (± 0.2) Hz, again indicating that the water attenuation has not suffered long-term variations
12 significant enough to negatively impact detector performance. So long as the background rate is stable, the
13 WBWC can be sensitive to increases in neutron emission rate as small as 0.88 Hz (to 3σ), allowing for low
14 rates of gamma ray emission, such as from the ^{137}Cs and ^{60}Co sources used here. The minimum detectable
15 source activity is therefore 3.1 neutrons per second assuming 28% absolute detector efficiency.

16



17

18

19

20

21

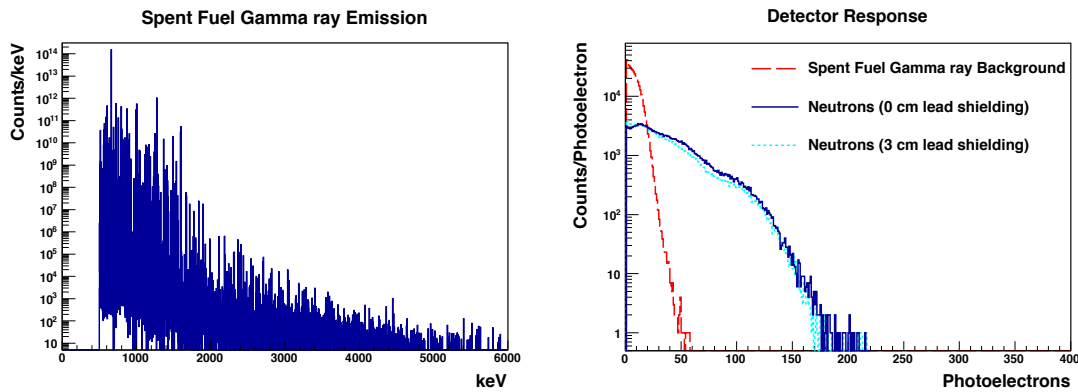
Figure 7: The detector response to the no source background is shown for a pair of one-hour data acquisitions taken on November 6 and January 15. The small difference between the two background runs indicates that the spectral response of the detector is very stable over long time scales.

Dazeley, S

Deleted: I

Dazeley, S

Deleted: I



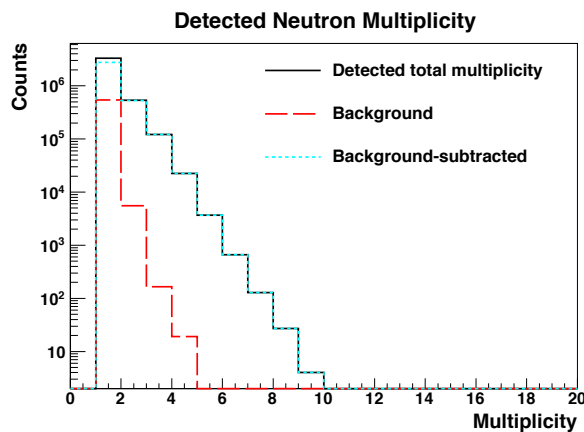
1
2 Figure 8: The gamma ray emission spectrum from a single 20cm spent fuel pin with burnup of 30 GWd/ton and
3 cooling time of 20 years (left). The simulated detector response to this source with 3cm of lead shielding inside
4 the source cavity is shown at right. The neutron capture detector response for an arbitrary number of neutrons
5 is also shown for comparison, with and without 3 cm of lead shielding.

6
7 To summarize, water Cherenkov detectors can provide sufficient energy resolution to discriminate between
8 neutron capture events and low energy gamma ray events. By selecting neutrons on the basis of their
9 detector spectral response alone, the WBWC can achieve an absolute neutron efficiency of 28% while
10 removing very close to 100% of the background from a ^{60}Co source (which we use here as a proxy for
11 gamma ray background associated with a fission source). We include all the neutrons emitted by the
12 fission source in our efficiency estimate, not simply the neutrons incident on the detector walls. The ^{60}Co
13 rejection factor at this efficiency is approximately 10^8 to 1. Remarkably, this is competitive with ^3He -based
14 detection. Discrimination against lower energy gamma rays from a ^{137}Cs source is even better.

15
16 To demonstrate the utility of the WBWC in the presence of very high gamma ray backgrounds, such as
17 spent fuel measurements, three factors remain to be studied. Firstly, no gamma ray shielding was used to
18 reduce detector susceptibility to high intensity gamma ray sources. Low energy gamma ray susceptibility
19 can be expected to be reduced further by such a shielding layer, with perhaps some loss of neutron
20 efficiency. Secondly, unlike common ^3He -based detectors of this type, our detector is monolithic.
21 Segmentation may be exploited in the future to further reduce the detector's overall susceptibility to high
22 gamma ray source rates. Since each segment would only need to contend with a fraction of the background
23 rate of a monolithic detector. Thirdly, unlike our ^{60}Co spent fuel proxy, a real spent fuel sample would
24 produce some high-energy gamma rays ($> \sim 5$ MeV). To predict the detector response to a real world spent
25 fuel sample we used a gamma ray emission model from the NGSF spent fuel library number 2,

1 (<http://www.lanl.gov/orgs/ndo/n4/documents/sfl2a.zip>), and modeled the response of the WBWC with the
2 tuned GEANT4 detector simulation. In **Figure 8** (left) we show the gamma ray emission spectrum used as
3 input to our model. This represents an integrated 900-second gamma ray source spectrum from a 20cm
4 long fuel pin subjected to a burnup of 30 GWd/ton and a cooling time of 20 years. Note that the most
5 intense emission line, by two orders of magnitude, is ^{137}Cs at 662 keV, and the range of intensities extend
6 over 14 orders of magnitude. The modeled detector response to these emissions is shown in **Figure 8**
7 (right), assuming 3cm of lead shielding inside the source cavity. For comparison the neutron capture
8 spectral response for an arbitrary number of neutron captures is also shown, with and without 3cm lead
9 shielding. The simulation suggests that the 3 cm of lead shield would only produce a small effect on the
10 neutron efficiency. The effect of pileup resulting from an intense flux of low energy gamma rays is
11 investigated in the next section. However, ignoring these effects for now, the spent fuel gamma ray rate
12 from our simulated spent fuel source that passes the neutron selection cut (50-200 photoelectrons) was less
13 than 10 Hz.

14
15
16
17



18
19 Figure 9: The detected neutron multiplicity for a one-hour $1.0 \mu\text{Ci } ^{252}\text{Cf}$ data acquisition compared with background.
20 The background subtracted ^{252}Cf multiplicity is also shown. See text for definitions.

21 In all of the following the above neutron selection cut is applied by default, **Figure 9** shows the detected
22 multiplicity from a one-hour data acquisition with the $1.0 \mu\text{Ci } ^{252}\text{Cf}$ source (black), compared to a one-hour
23 no source background run (light blue). The background-subtracted multiplicity is also shown in dark blue.
24 We group any two neutron-like events into the same multiplicity set if they fall within $50 \mu\text{s}$ of each other.

25

1

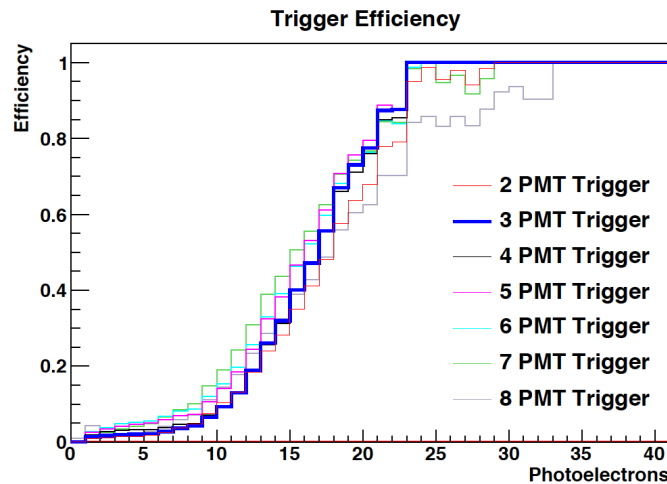
2 4. Detector Performance in the Presence of Intense Gamma Ray Activity

3

4 Until now we have only considered neutron/gamma ray discrimination on an event-by-event basis, at rates
5 consistent with little to no pileup. Here we consider performance effects that may result from very high
6 rates of low energy gamma ray emission, such as from a spent fuel source. Even if gamma ray background
7 is not energetic enough to trigger the detector, extremely high rates can produce an almost continuous level
8 of background light inside the detector, which may impact the efficiency and/or spectral response of the
9 PMTs at higher energies. In anticipation of these effects we attempted an optimization of our trigger.

10 **Figure 10** shows the detector efficiency as a function of digitized light level (number of photoelectrons)
11 for a selection of PMT trigger multiplicities. The efficiencies were calculated using the ratio of the two
12 curves shown in Figure 5 for each of the trigger multiplicities. The steepest curve, and hence the most
13 efficient trigger, was a trigger multiplicity of three, shown in bold blue. We employed this trigger
14 condition in the following.

15



16

17

18

Figure 10: the detector trigger efficiency as a function of detected light (photoelectrons) for a variety of trigger multiplicities. The steepest curve (PMT Multiplicity=3), and hence the most efficient trigger, is shown in bold.

19

20

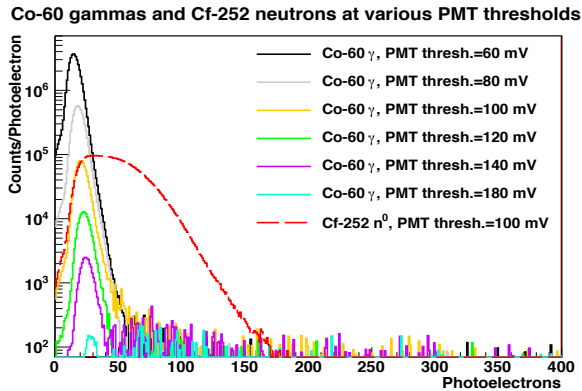
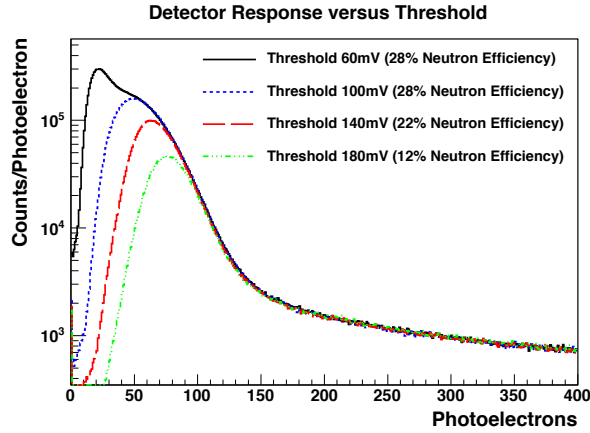


Figure 11: A series of one-hour ^{60}Co background subtracted runs with increasing trigger thresholds. Also shown for comparison is the neutron capture spectrum from a one-hour ^{252}Cf run at a high PMT threshold of 100mV.

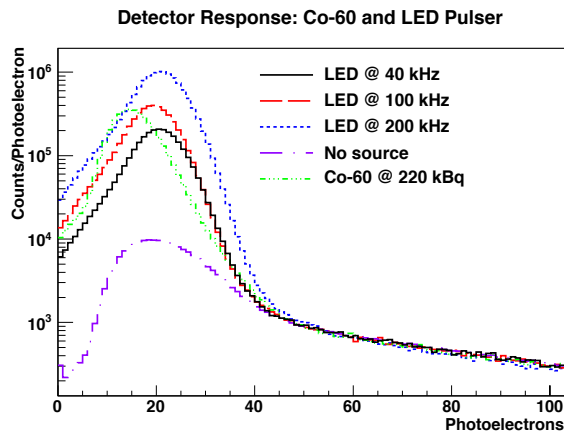
1
2
3
4
5
6
7
8
9
10
11
12
13
14
15
16
17

Figure 11 shows the spectral response as a function of PMT discriminator threshold for a set of one-hour background subtracted ^{60}Co data acquisitions. For reference, all the spectra shown previously were obtained with a relatively low nominal threshold setting of 60mV per PMT. Our motivation was to find a threshold setting that eliminates ^{60}Co events, and then to test its utility for fission sources that included an intense background gamma ray component. The ^{60}Co trigger rate at 100mV is approximately the same as the 60mV no-source trigger rate. We also show for reference the spectral response of the ^{252}Cf source at the 100mV threshold. Note that the peak of this distribution is now at approximately 50 photoelectrons. Note also that the background-subtracted ^{60}Co signal drops to near zero at a trigger threshold of 180 mV. The best trigger level for the application will need to be adjusted as needed if background levels are high. If the source to be investigated has low gamma ray activity the threshold can be set low in order to maximize neutron efficiency.



1
2
3
4
5
6
7
8
9
10
Figure 12: The spectral response of the detector to a ^{252}Cf source for various PMT threshold settings. The resulting neutron detection efficiencies at each threshold are also shown.

Figure 12 shows the detector response to ^{252}Cf as a function of the PMT threshold. Based on the trigger threshold absolute efficiency of 28% defined earlier with the analysis threshold of 50 photoelectrons, the absolute efficiencies at higher thresholds were calculated from the relative changes in the integrated detection rate at each PMT threshold.

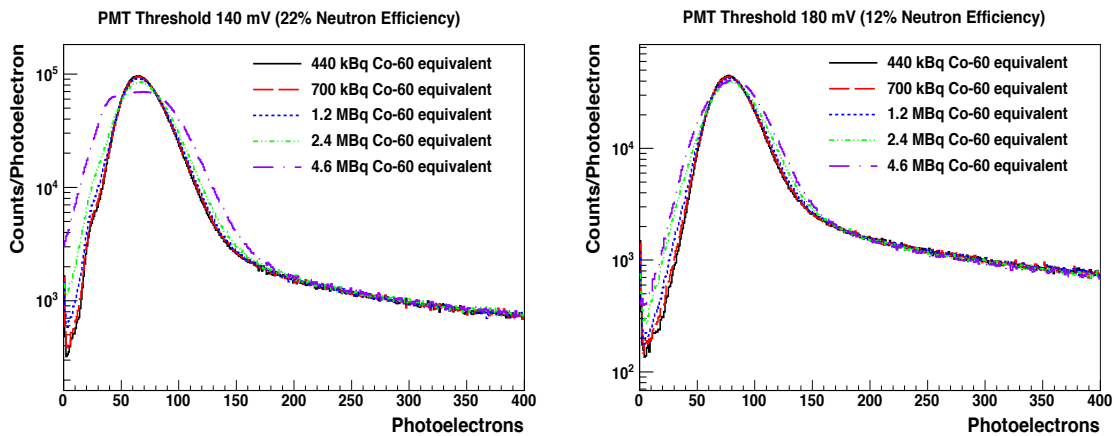


11
12
13
14
15
16
17
18
19
20
Figure 13: An investigation of the equivalence, in terms of detector response, of an LED pulser operating at different frequencies and a 220 kBq ^{60}Co source. The LED bias was set to 0.88 volts. For this bias, a 100 kHz LED rate models the energy output of a ^{60}Co source reasonably well, especially at the high-energy tail near 50 photoelectrons.

The question of neutron efficiency and detector response as a function of very high levels of low energy gamma ray background is a very important one for any technique in this field. In principle, the Cherenkov light output from gamma rays less than about 1 MeV should be small, as the resulting Compton scattered electrons are generally only slightly above the Cherenkov threshold. The use of both fresh and spent fuel

1 samples was outside the scope of this study. However, we experimentally modeled the presence of a
 2 fission source with an intense gamma ray component by a combining multiple sources as proxies for a high
 3 activity gamma ray source – a low intensity ^{60}Co source, a green LED mounted inside the detector, and the
 4 $1\ \mu\text{Ci}\ ^{252}\text{Cf}$ source. The first task was to find an LED bias voltage (i.e. light intensity per pulse) that closely
 5 matches the detector response obtained from the ^{60}Co source. **Figure 13** shows the detector response
 6 obtained using the optimum bias in our case (60 nanosecond pulses at 0.88 volts). The ^{60}Co source at 220
 7 kBq provides a trigger rate and energy spectrum approximately similar to the LED pulsing at 100 kHz. In
 8 similar fashion to the detector response to ^{60}Co , the upper edge of the LED spectrum falls off at
 9 approximately 50 photoelectrons.

10



11

12 **Figure 14:** The detector spectral response for one-hour ^{252}Cf data acquisitions in the presence of progressively
 13 more intense low energy background. The ^{60}Co equivalent rates were modeled by combining a ^{60}Co source and a
 14 pulsing LED. We show the effect for two different PMT trigger thresholds, 140 mV and 180 mV, corresponding
 15 to 22% and 12% neutron efficiency respectively.

16

17

18

Figure 14 shows the detector spectral response to the $1.0\ \mu\text{Ci}\ ^{252}\text{Cf}$ source as a function of different

19

low energy background intensities. The ^{60}Co and LED related backgrounds were all below threshold,

20

however, even when low energy backgrounds are not energetic enough to trigger the detector on an

21

event-by-event basis, pileup may degrade the energy resolution of the detector at higher energies.

22

This pileup may arise when the rate of low energy gamma-rays is so high as to create a small

23

amplitude, but nearly constant ‘wash’ of Cherenkov light, superimposed on the Cherenkov light

24

created by real neutron captures. Recall that at low background intensities, an analysis cut at 50

25

photoelectrons rejects nearly all of the ^{60}Co gamma rays. At high intensities however, we reject these

1 events with the trigger so as not to saturate the DAQ. We tested two high PMT threshold settings –
 2 140 mV and 180mV, corresponding to neutron efficiencies of 22% and 12% respectively. The various
 3 high intensity backgrounds were modeled by varying the LED rate in combination with the fixed ^{60}Co
 4 source. The ^{60}Co equivalent rates were calculated assuming the conversion calculated above (100
 5 kHz LED \approx 220 kBq ^{60}Co). We observed reasonably consistent detector response (resolution and
 6 efficiency) at ^{60}Co equivalent background levels up to \sim 4 MBq. If, as before, we accept events
 7 between 50 and 200 photoelectrons as neutron candidates, the neutron count rate at each
 8 background level is given in Table 1. The data indicate that neutron detection efficiency is consistent
 9 to within 5% up to a ^{60}Co equivalent source intensity of \sim 4 MBq. Note also that the lower threshold
 10 (140 mV), capable of 22% neutron efficiency, is as effective at providing neutron detection
 11 consistency over a large range of background intensities as the higher threshold setting (180 mV).

12
 13 [Table 1: Measured neutron detection rate for steadily increasing rates of \$^{60}\text{Co}\$ equivalent background source](#)
 14 [intensity.](#)

^{60}Co Equivalent Background Rate	Neutron Detection Count rates (Hz)	
	140 mV threshold (22% neutron efficiency)	180 mV threshold (12% neutron efficiency)
440 kBq	965 Hz	478 Hz
700 kBq	965 Hz	480 Hz
1.2 MBq	964 Hz	485 Hz
2.4 MBq	968 Hz	493 Hz
4.6 MBq	1010 Hz	558 Hz

15

16

17 5. Discussion and Conclusions

18 In the following we evaluate the performance of the WBWC relative to existing ^3He techniques using the
 19 safeguards figure-of-merit (FOM) defined earlier for two scenarios, the NDA of a fresh fuel SNM sample
 20 without a significant high-energy gamma ray emission rate and the NDA of a spent fuel sample with a high
 21 gamma ray emission rate. For fresh fuel samples with low rates of gamma ray emission, the most
 22 significant backgrounds come from high-energy gamma rays incident on the detector from the local
 23 environment and high-energy cosmogenic muons and gamma rays. For this detector, we select neutron
 24 capture events on the basis of the detector response, between 50 and 200 photoelectrons. We have shown

1 that the counter has a neutron detection efficiency of 28% with this selection criterion. The neutron capture
2 time, or die-away time is 16 μ s. The neutron selection criterion almost entirely eliminates low energy
3 gamma rays (\sim 2 MeV) incident on the detector, whether they be from the local environment, or from
4 radioactivity in the source under investigation (see Figure 4 and 6). The remaining non-source
5 backgrounds are primarily due to cosmic ray particles such as muons, neutrons and gammas, or neutrons
6 from the local environment. Fortunately these backgrounds can be measured very accurately given the
7 stable detector performance demonstrated over time periods of three months.

8

9 The safeguards FOM for the WBWC is

10

11
$$FOM = \frac{28}{\sqrt{16}} = 7.0$$

12

13 This compares favorably with alternative systems such as the Boron plate detector of [18] (FOM = 2.74),
14 and the ^3He -based HLNCC-II detector, a safeguards standard employed by many nuclear facilities and the
15 IAEA [19] (FOM = 2.67). The FOM here is higher primarily because of the efficiency is relatively high,
16 but also because the neutron capture time is short. The relatively high value of the FOM suggests that the
17 WBWC might be the ideal detector technology in circumstances where source related background is in the
18 medium to low range.

19

20 For spent fuel samples, or any sample that emits very intense gamma ray backgrounds, a higher trigger
21 threshold might be utilized, so as to avoid digitizing too much background. As we have shown, the WBWC
22 was able to maintain a neutron efficiency of $22 \pm 1\%$ in the presence of gamma ray backgrounds equivalent
23 to approximately 4 MBq of ^{60}Co . The FOM for intense gamma ray sources such as these is nevertheless
24 still very competitive – 5.5. For water Cherenkov systems, the level of background gamma ray
25 susceptibility is highly dependent on energy. Lower energy gamma rays, such as from ^{137}Cs produce
26 almost no response when compared to ^{60}Co . This is because the Cherenkov process in water is very
27 nonlinear in the energy region between 0.5 and 1.5 MeV. A question arises as to how best to evaluate the
28 effectiveness of various detection techniques in a consistent way, accounting for realistic background

1 conditions. A water Cherenkov detector is likely to compare more favorably with detectors evaluated for
2 their susceptibility to background ^{137}Cs gamma rays, while less so for ^{60}Co . Both comparisons are common
3 in the literature (e.g. [6][7]). For this reason future studies of this technology will focus less on background
4 proxies such as ^{137}Cs , ^{60}Co and pulsing LEDs, in favor of real uranium and plutonium samples, including
5 fresh and spent fuel.

6

7 In conclusion, the WBWC evaluated here has an absolute neutron detection efficiency of approximately
8 28% and a FOM of 7.0. The efficiency was confirmed to within 0.5% using two independent methods. The
9 counter has very limited susceptibility to low energy gamma ray backgrounds such as ^{137}Cs and ^{60}Co . We
10 demonstrated a ^{60}Co rejection factor of $\sim 10^8$ to 1, for activities ≤ 220 kBq. For sources with higher
11 background activities the WBWC demonstrated consistent neutron detection efficiencies of $22 \pm 1\%$ (FOM
12 5.5), up to ^{60}Co -like source activities of approaching 4 MBq. In the near future we hope to be able to test
13 the WBWC with real world fission sources such as uranium and plutonium samples.

14

15 | 6. Acknowledgements

16 We would like to thank Darrell Carter for his expert technical help with both the detector design and
17 construction and John Steele for programming the trigger logic in the FPGA. This work was performed
18 under the auspices of the US Department of Energy by Lawrence Livermore National Laboratory under
19 Contract DE-AC52-07NA27344, Release no. LLNL-JRNL-xxxxxx. The authors wish to thank the DOE
20 NA-22 for their support of this project.

21

[1] R. T. Kouzes, "The ^3He Supply Problem", PNNL-18388, (2009)

[2] T. M. Persons and G. Aloise, "Neutron detectors: Alternatives to using helium-3", Government Accountability Office Technology Assessment, Report to Congress, (2011)

[3] D. A. Shea, D. Morgan, "The Helium-3 Shortage: Supply, Demand and Options for Congress", Congressional Research Service, (2010)

[4] A. Prosdocimi, "Non-destructive assay of fissile materials by detection and multiplicity analysis of spontaneous neutrons" nuclear science and technology, 1979.

[5] N. Ensslin, M. Krick, M. Pickrell, D. Reilly, J. Stewart "Chapter 6. Passive Neutron Multiplicity Counting", Passive Nondestructive Assay of Nuclear Materials – 2007 Addendum, Los Alamos National Laboratory Report, LA-UR-07-1402 (2007)

[6] D. Henzlova, L.G.Evans, H.O.Menlove, M.T.Swinhoe, J.B.Marlow, "Experimental evaluation of a boron-lined parallel plate proportional counter for use in nuclear safeguards coincidence counting", Nucl. Inst. and Meth. A. V697 (2013), P114

-
- [7] A.P. Simpson, S. Jones, M.J. Clapham and S. A. McElhane, "A Review of Neutron Detection Technology Alternatives to Helium-3 for Safeguards Applications", INMM 52nd Annual Meeting (2011)
- [8] D. Reilly, N. Ensslin, H. Smith, Jr., and S. Kreiner, "Passive Nondestructive Assay of Nuclear Materials (PANDA)", Los Alamos National Laboratory Report, LA-UR-90-732.
- [9] H.O. Menlove, R.J. Dickinson, I. Douglas, C. Orr, F.J.G. Rogers, G. Wells, R. Schenkel, G. Smith, A. Fattah, A. Ramalho, "Field Test and Calibration of Neutron Coincidence Counters for High-Mass Plutonium Samples", Los Alamos National Laboratory Report, LA-10815-MS.
- [10] S. Dazeley, A. Bernstein, N.S. Bowden, R. Svoboda, "Observation of neutrons with a Gadolinium doped water Cherenkov Detector", Nucl. Inst. and Meth.,A, V607 (2009), P616
- [11] M. Sweany, A. Bernstein, N.S. Bowden, S. Dazeley, G. Keefer, R. Svoboda, M. Tripathi, "Large-scale gadolinium-doped water Cherenkov detector for nonproliferation", V654, (2011), P377
- [12] S. Dazeley, M. Sweany, A. Bernstein, "SNM detection with an optimized water Cherenkov neutron detector", V693, (2012), P148
- [13] W. Coleman, A. Bernstein, S. Dazeley, R. Svoboda, "Transparency of 0.2% GdCl₃ doped water in a stainless steel test environment", Nucl. Inst. and Meth. A. V595 (2008), P339
- [14] S. Agostinelli, et al., Nuclear Instruments and Methods A 506 (2003) 250.
- [15] J. Allison, et al., IEEE Transactions on Nuclear Science NS-53 (1) (2006) 270.
- [16] <<http://Geant4.cern.ch>>
- [17] Y. Fukuda et al., "The Super-Kamiokande Detector", Nucl. Inst. and Meth.,A, V501 (2003), P418
- [18] D. Henzlova, H. O. Menlove, M. T. Swinhoe, J. B. Marlow, "Design and Development of a Safeguards Coincidence Counter Based on Boron-lined Proportional Detector Technology - High Level Neutron counter Boron (HLNB)", Los Alamos National Laboratory Report, LA-UR-12-26261.
- [19] Menlove H.O., Swansen J.E.; A high-performance neutron time correlation counter", Nuclear Technology 71, 497, (1985)